

Cosmic ray velocity and electric charge measurements with the AMS/RICH detector: prototype results

Luísa Arruda, Fernando Barão, Patrícia Gonçalves, Rui Pereira

LIP/IST

Av. Elias Garcia, 14, 1^o andar

1000-149 Lisboa, Portugal

e-mail: luisa@lip.pt

arXiv:0801.4952v1 [astro-ph] 31 Jan 2008

Abstract—The Alpha Magnetic Spectrometer (AMS) to be installed on the International Space Station (ISS) will measure charged cosmic ray spectra of elements up to iron, in the rigidity range from 1GV to 1TV, for at least three years. AMS is a large angular spectrometer composed of different subdetectors, including a proximity focusing Ring Imaging Čerenkov (RICH) detector. This will be equipped with a mixed radiator made of aerogel and sodium fluoride (NaF), a lateral conical mirror and a detection plane made of 680 photomultipliers coupled to light guides. The RICH detector allows measurements of particle's electric charge up to iron, and particle's velocity. Two possible methods for reconstructing the Čerenkov angle and the electric charge with the RICH will be discussed.

A RICH prototype consisting of a detection matrix with 96 photomultipliers, a segment of a conical mirror and samples of the radiator materials was built and its performance was evaluated using ion beam data. Results from the last test beam performed with ion fragments resulting from the collision of a 158 GeV/c/nucleon primary beam of indium ions (CERN SPS) on a lead target are reported. The large amount of collected data allowed to test and characterize different aerogel samples and the NaF radiator. In addition, the reflectivity of the mirror was evaluated. The data analysis confirms the design goals.

I. THE AMS-02 EXPERIMENT

The Alpha Magnetic Spectrometer [1] (AMS) is a particle detector to be installed in the International Space Station (ISS) for at least three years. The spectrometer will be able to measure the rigidity ($R = pc/Z\beta$), the charge (Z), the velocity (β) and the energy (E) of cosmic rays from some MeV up to 1 TeV within a geometrical acceptance of $0.5 \text{ m}^2 \cdot \text{sr}$. Figure I shows a schematic view of the AMS spectrometer. At both ends of the AMS spectrometer exist the Transition Radiation Detector (TRD) (top) and the Electromagnetic Calorimeter (ECAL) (bottom). Both will provide AMS with capability to discriminate between leptons and hadrons. Additionally the calorimeter will trigger and detect photons. The TRD will be followed by the first of the four Time-of-Flight (TOF) system scintillator planes. The TOF system [4] is composed of four roughly circular planes of 12 cm wide scintillator paddles, one pair of planes above the magnet, the upper TOF, and one pair below, the lower TOF. There will be a total of 34 paddles. The TOF will provide a fast trigger within 200 ns, charge and velocity measurements

for charged particles, as well as information on their direction of incidence. The TOF operation at regions with very intense magnetic fields forces the use of shielded fine mesh phototubes and the optimization of the light guides geometry, with some of them twisted and bent. Moreover the system guarantees redundancy, with two photomultipliers on each end of the paddles and double redundant electronics. A time resolution of 140 ps for protons is expected [4].

The tracking system will be surrounded by veto counters and embedded in a magnetic field of about 0.9 Tesla produced by a superconducting magnet. It will consist on a Silicon Tracker [3], made of 8 layers of double sided silicon sensors with a total area of 6.7 m^2 . There will be a total of 2500 silicon sensors arranged on 192 ladders. The position of the charged particles crossing the tracker layers is measured with a precision of 10 μm along the bending plane and 30 μm on the transverse direction. With a bending power (BL^2) of around $0.9 \text{ T} \cdot \text{m}^2$, particles rigidity is measured with an accuracy better than 2% up to 20 GV and the maximal detectable rigidity is around 1-2TV. Electric charge is also measured from energy deposition up to $Z = 26$.

The Ring Imaging Čerenkov Detector (RICH) [2] will be located right after the last TOF plane and before the electromagnetic calorimeter. It will be described in detail in next section.

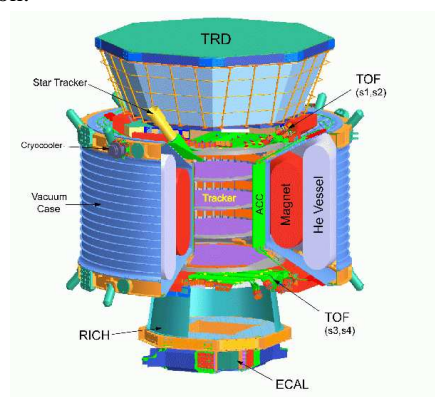


Fig. 1. A whole view of the AMS Spectrometer.

The long stay of AMS in space and its large acceptance will allow the accumulation of a large statistic of events increasing in several orders of magnitude the sensitivity of the proposed physical measurements. With an average collection rate of 1000 events per second, a total of 10^9 protons per year and around 10^4 antiprotons will be accumulated.

The main goals of the AMS-02 experiment are:

- A precise measurement of the charged cosmic ray spectrum between 100 MeV and 1 TeV, and the detection of photons up to a few hundred GeV;

- A search for heavy antinuclei ($Z \geq 2$), which if discovered would signal the existence of primordial antimatter;

- Search for non-baryonic dark matter through the detection of annihilation products appearing as anomalies of the cosmic-ray spectra (e^+ , p , \bar{p} and d);

II. THE AMS RICH DETECTOR

The RICH is a proximity focusing device with a dual radiator configuration on the top made of 92 aerogel 25 mm thick tiles with a refractive index 1.050 and sodium fluoride (NaF) tiles with a thickness of 5 mm in the center covering an area of $34 \times 34 \text{ cm}^2$. The NaF placement prevents the loss of photons in the hole existing in the center of the readout plane ($64 \times 64 \text{ cm}^2$), in front of the ECAL calorimeter located below. The radiator tiles are supported by a 1 mm thick layer of methacrylate ($n=1.5$) free of UV absorbing additives.

The detection matrix is composed of 680 multipixelized photon readout cells each consisting of a photomultiplier coupled to a light guide, HV divider plus front-end (FE) electronics, all housed and potted in a plastic shell and then enclosed in a magnetic shielding with a thickness varying from 0.8 to 1.2 mm. The photon detection is made with an array of multianode Hamamatsu tubes (R7600-00-M16) with a spectral response ranging from 300 to 650 nm and a maximum quantum efficiency at 420 nm. To increase the photon collection efficiency, a light guide consisting of 16 solid acrylic pipes glued to a thin top layer (1 mm) was produced. It is optically coupled to the active area of phototube cathode through a 1 mm flexible optical pad. With a total height of 31 mm and a collecting surface of $34 \times 34 \text{ mm}^2$, it presents a readout pixel size of 8.5 mm and a pitch of 37 mm. The light guide is mechanically attached through nylon wires to the photomultiplier polycarbonate housing.

A high reflectivity conical mirror surrounds the whole set. The mirror was included to increase the device acceptance since around 33% of the aerogel generated photons impact on the mirror. It consists of a carbon fiber reinforced composite substrate with a multilayer coating made of aluminium and SiO_2 deposited on the inner surface. This ensures a reflectivity higher than 85% for 420 nm wavelength photons.

The RICH has a truncated conical shape with an expansion height of 46.3 cm, a top radius of 60 cm and a bottom radius of 67 cm. The total height of the detector is 60.5 cm and it covers 80% of the AMS magnet acceptance. Figure 2 shows a schematic view of the RICH detector.

RICH was designed to measure the velocity ($v \approx c$) of singly charged particles with a resolution $\Delta v/v$ of 0.1%, to extend the charge separation (Z) up to iron ($Z=26$), to contribute to e^-p separation and to albedo rejection.

In order to validate the RICH design, a prototype with an array of 9 \times 11 cells filled with 96 photomultiplier readout units similar to part of the matrix of the final model was constructed. The performance of this prototype has been tested with cosmic muons and with a beam of secondary ions at the CERN SPS produced by fragmentation of a primary beam in 2002 and 2003. The light guides used were prototypes with a slightly smaller collecting area ($31 \times 31 \text{ mm}^2$). Different samples of the radiator materials were tested and placed at an adjustable supporting structure. Different expansion heights were set in order to have fully contained photon rings on the detection matrix like in the flight design. A segment of a conical mirror with 1/12 of the final azimuthal coverage, which is shown in left picture of Figure 3, was also tested.

The RICH assembly has already started at CIEMAT in Spain and is foreseen to be finished in July 2007. A rectangular grid has already been assembled and has been subject to a mechanical fit test, functional tests, vibration tests and vacuum tests. The other grids will follow. The refractive index of the aerogel tiles is being measured and the radiator container was subjected to a mechanical test. The final integration of RICH in AMS will take place at CERN in 2008.

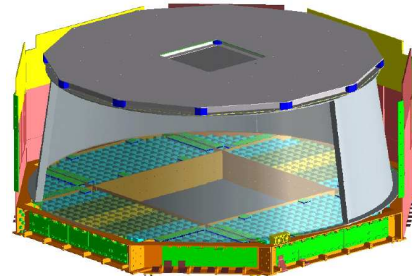


Fig. 2. Schematic view of the RICH detector.

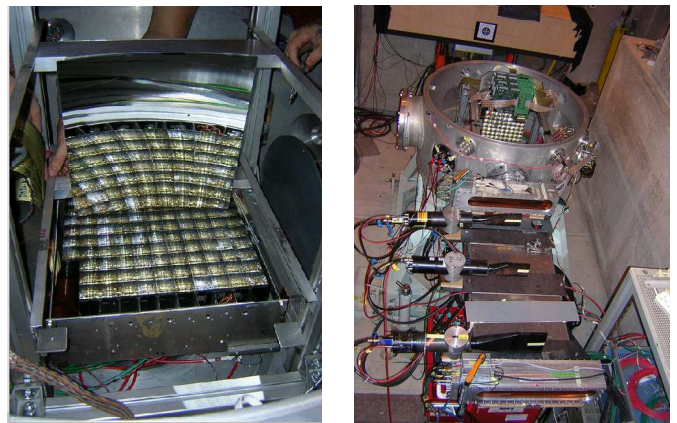


Fig. 3. Prototype with reflector (left). Top view of the test beam 2003 experimental setup using CERN SPS facility (right).

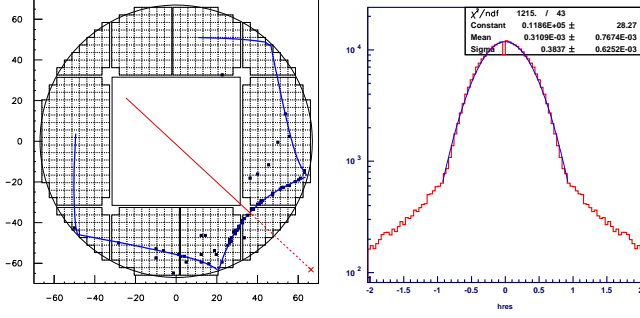


Fig. 4. Beryllium event display generated in a NaF radiator. The reconstructed photon pattern (full line) includes both reflected and non-reflected branches. The outer circular line corresponds to the lower boundary of the conical mirror. The square is the limit of the non-active region (left). Hit's residuals distribution belonging to photon rings generated in an aerogel radiator, $n=1.05$, 2.5 cm thick.

III. BETA (β) AND CHARGE (Z) RECONSTRUCTION

A charged particle crossing a dielectric material of refractive index n with a velocity β , greater than the speed of light in that medium, emits photons. The aperture angle of the emitted photons with respect to the radiating particle is known as the Čerenkov angle, θ_c , and it is given by (see Ref. [5])

$$\cos \theta_c = \frac{1}{n\beta} \quad (1)$$

It follows that the velocity of the particle, β , is straightforwardly derived from the Čerenkov angle reconstruction, which is based on a fit to the pattern of the detected photons. Complex photon patterns can occur at the detector plane due to mirror reflected photons, as can be seen on the left display of Figure 4. The event shown is generated by a simulated beryllium nucleus crossing the NaF radiator. The Čerenkov angle reconstruction procedure relies on the highly accurate information (see Section I) of the particle direction (θ, ϕ) provided by the tracker. The tagging of the hits signaling the passage of the particle through the solid light guides in the detection plane provides an additional track element, however, those hits are excluded from the reconstruction. The best value of θ_c will result from the maximization of a Likelihood function, built as the product of the probabilities, p_i , that the detected hits belong to a given (hypothetical) Čerenkov photon pattern ring,

$$L(\theta_c) = \prod_{i=1}^{N_{\text{hits}}} p_i^{s_i} [r_i(\theta_c)] \quad (2)$$

This probability takes into account r_i , the closest distance of the hit to the Čerenkov pattern and s_i the signal strength. The probability of a hit belonging to the pattern is obtained by taking into account that it can either be part of the noise (essentially flat) or of the Čerenkov pattern (Gaussian distributed). Expressing b as the photon background fraction, D as the detector's dimensions and w as the width of the residuals distribution (as can be seen in right plot of Figure 4), we can write:

$$p_i = (1 - b)G(\theta_c; r_i) + \frac{b}{D} \quad (3)$$

where $b = 0.5122$ and 0.105 respectively for aerogel and NaF in the prototype setup. The detector's dimension is defined as $D=100$ cm for flight setup and 20 cm for prototype setup. For a more complete description of the method see Ref. [5].

The Čerenkov photons produced in the radiator are uniformly emitted along the particle path inside the dielectric medium, L , and their number per unit of energy depends on the particle's charge, Z , and velocity, β , and on the refractive index, n , according to the expression:

$$\frac{dN}{dE} = \frac{Z^2 L}{c} \left(1 - \frac{1}{\beta^2 n^2} \right) \quad (4)$$

Therefore to reconstruct the charge the following procedure is required:

Čerenkov angle reconstruction.

Estimation of the particle path, L , which relies on the information of the particle direction provided by the tracker.

Counting the number of photoelectrons. The number of photoelectrons related to the Čerenkov ring has to be counted within a fiducial area, in order to exclude the uncorrelated background. In particular it ensures the exclusion of photons which are scattered in the radiator. A distance of 13 mm to the ring was defined as the limit for photoelectron counting, corresponding to a ring width of 5 pixels.

Evaluation of the photon detection efficiency. The number of radiated photons (N) which will be detected ($n_{p,e}$) is reduced due to the interactions with the radiator (ϵ_{rad}), the photon ring acceptance (ϵ_{geo}), light guide efficiency (ϵ_{lg}) and photomultiplier efficiency (ϵ_{pmt}).

$$n_{p,e} = N \epsilon_{\text{rad}} \epsilon_{\text{geo}} \epsilon_{\text{lg}} \epsilon_{\text{pmt}} \quad (5)$$

The charge is then calculated according to expression 4, where the normalization constant can be evaluated from a calibrated beam of charged particles. For a more complete description of the charge reconstruction method see Ref. [5].

IV. RESULTS WITH THE RICH PROTOTYPE

The RICH prototype was subject to cosmic muons and to in-beam tests using secondary nuclei from fragmentation of 20 GeV/c/nucleon lead (Pb) ions in a beryllium target and 158 GeV/c/nucleon indium nuclei in a Pb target from the CERN SPS in 2002 and 2003, respectively [6].

In 2003 a monochromatic particle beam with a momentum resolution 0.15% $\Delta P/P = 1.5\%$ was obtained. The optics of the line was tuned to provide a beam as parallel as possible, with a divergence less than 1 mrad. The beam section was 1 mm² for the narrow beam runs and 1 cm² for the spread beam runs.

The beam nuclear composition could be selected according to the desired A/Z value of the fragmentation products by setting the beam line rigidity at the appropriate value. Three main selection values were established: $A/Z=2$ (⁴He, ⁶Li, ¹⁰B, ¹²C,...); $A/Z=2.25$ to enhance the ⁹Be peak and $A/Z=2.35$ to enhance the indium peak.

Figure 3 (right) shows a general view of the 2003 test beam setup in the experimental area H8-SPS at CERN. The prototype was placed inside a light-tight container. The setup was completed with AMS silicon tracker layers placed upstream in the beam, a TOF prototype placed downstream, two multi-wire proportional chambers, two organic scintillator counters and during a certain period a plastic Čerenkov counter. The two scintillators placed 1 m apart in front of the prototype container, provided the DAQ trigger as well as an independent charge measurement. The silicon tracker prototype provided a very precise measurement of the particle track parameters for the event reconstruction as well as an external selection of charge.

The purposes of the tests were testing flight front-end electronics, characterize the performance of the aerogel and the NaF radiators, estimating the mirror reflectivity and evaluating the global functionality of the prototype. A total number of 11 million events were recorded during eleven days. Different particle incidences were obtained by rotating the prototype setup with respect to the beam line ($0^\circ, 5^\circ, 10^\circ, 15^\circ, 20^\circ$).

The event selection was mainly intended to remove wrongly reconstructed tracks, events with clusterized hits and events arising from later fragmentation. First, consistency between the external determination of the track transverse coordinates and the estimation from the reconstructed ring is required. Then events with more than one particle cluster in the detection matrix are rejected. Furthermore, the Kolmogorov probability of the event is calculated requiring an uniform azimuthal distribution of the ring hits.

The evaluation of the aerogel samples in order to make a final radiator choice was one of the key issues of these tests. Different production batches from two manufacturers, Matsushita Electric Co. (MEC) and Catalysis Institute of Novosibirsk (CIN) with different refractive indexes, 1.03 and 1.05, were analyzed. The required criteria for a good candidate were a high photon yield, in order to ensure a good ring reconstruction efficiency and accurate β and charge measurements.

The aerogel light yield depends on the tile thickness and on its optical properties (refractive index and clarity). The light yield has been evaluated from the analysis of helium samples collected in 2003 and from the analysis of proton data samples gathered in 2002 with different beam momentum between 5 and 13 GeV/c [7].

Figure 5 (left) shows the evolution of the light yield of the different aerogel samples tested in 2002 with the proton beam momentum. A fit to each set of data was applied and the light yield for a proton with $\beta = 1$, generating fully contained rings in a radiator with a common thickness of 3 cm was extrapolated. Right plot of the same figure shows the normalized to 3 cm thickness light yield for the different aerogel samples tested in 2002 and 2003. Two interesting features are enhanced. In one hand, the same sample of CINy02.103 was used in both years and its light yield analysis shows the same value which proves the setup stability and the aerogel good performance after one year period; on the other hand it is notorious the highest signal comes from a CIN

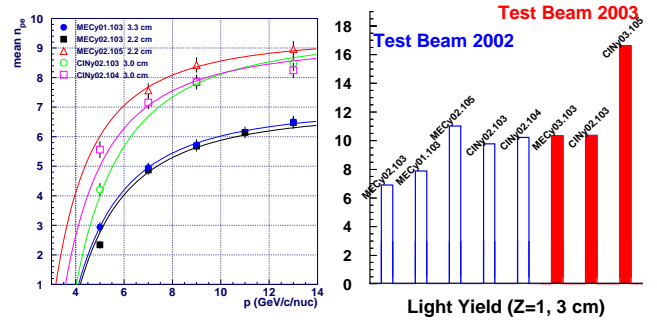


Fig. 5. Light yield as function of proton beam momentum for the different aerogel samples tested in 2002 (left). Light yield comparison based on test beam data 2002 and 2003. All values were extrapolated for fully contained rings generated by a particle with $\beta = 1$ and in an aerogel radiator with a common thickness of 3 cm (right).

sample produced in 2003 with 1.05 refractive index reflecting the very good clarity ($0.0055 \text{ m}^4/\text{cm}$) of the aerogel batch.

The resolution of the β measurement, obtained as explained in Section III, was estimated using a Gaussian fit to the reconstructed β spectrum, shown in left plot of Figure 6 for helium nuclei. Data were collected with the aerogel radiator CINy03.105, 2.5 cm thick together with an expansion height of 35.31 cm. The events shown correspond to particles inciding vertically and generating fully contained rings. The β reconstructed from a simulated helium data is also shown (shaded histogram) superimposed with good agreement between data and Monte Carlo.

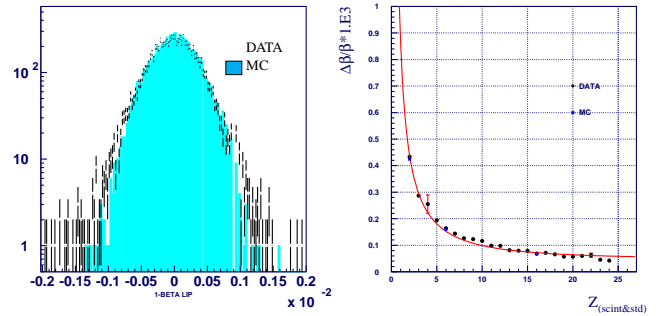


Fig. 6. Comparison of the $(\beta - 1)$ distribution for helium data (black dots) and simulation (shaded) (left). Evolution of the β resolution with the charge obtained for the same aerogel radiator. Simulated points for $Z=2, 6, 16$ are marked with full squares (right).

The charge dependence of the velocity relative resolution for the same radiator is shown in the right plot of Figure 6. The different charges were selected using external and independent measurements performed by the silicon tracker prototype and by the two scintillators. The observed resolution varies according to a law $\propto 1/Z$, as it is expected from the charge dependence of the photon yield in the Čerenkov emission, up to a saturation limit set by the pixel size of the detection unit cell. The function used to perform the fit is the following:

$$\Delta\beta/\beta = \frac{A}{Z} + B^2 \quad (6)$$

where, A means the β resolution for a singly charged particle while B means the resolution for a very high charge generating

a large number of hits, here the resolution is dominated by the pixel size as mentioned before. The fitted values are $A = 0.872 \pm 0.003$ and $B = 0.047 \pm 0.001$ for the run conditions stated above. Simulated data points for $Z=2, 6, 16$ are marked upon the same plot with full squares. Once more the agreement between data and Monte Carlo measurements for charges different of $Z=2$ is good.

The beta resolution for a $\beta = 1$, helium nuclei impacting in each of the aerogel samples tested in 2003 are summarized in Table I. The results are for a common expansion height extrapolated from the values measured at the adjusted heights.

All the tested radiators fulfill the RICH requirement for measurement.

resolution for $Z=2, H=33.5$ cm			
radiator	CIN103	MEC103	CIN105
() 10^3	0.421 0.003	0.435 0.002	0.459 0.004

TABLE I

BETA RESOLUTION FOR A HELIUM PARTICLE WITH $\beta = 1$ OBTAINED FOR ALL THE AEROGEL SAMPLES TESTED IN 2003 AND EXTRAPOLATED FOR A COMMON EXPANSION HEIGHT OF 33.5 CM.

The distribution of the reconstructed charges in an aerogel radiator of $n=1.05$, 2.5 cm thick is shown in left plot of Figure 7. The reconstruction method used was the one described in Section III. The spectrum enhances a structure of well separated individual charge peaks over the whole range up to iron ($Z=26$). This spectrum was measured for a beam selection of $A/Z=9/4$.

The charge resolution for each nuclei, shown in right panel of Figure 7, was evaluated through individual Gaussian fits to the reconstructed charge peaks selected by the independent measurements performed by the scintillators and silicon tracker detectors. A charge resolution for proton events slightly better than 0.17 charge units is achieved and as expected the best charge resolution is provided by this radiator due to its higher photon yield.

The charge resolution as function of the charge Z of the particle follows a curve that corresponds to the error propagation on Z which can be expressed as:

$$\sigma(Z) = \frac{1}{2} \sqrt{\frac{s}{N_0} + \frac{2}{N_{pe}} + Z^2 \frac{N}{N_{syst}}^2} : \quad (7)$$

This expression describes the two distinct types of uncertainties that affect Z measurement: the statistical and the systematic. The statistical term is independent of the nuclei charge and depends essentially on the amount of Čerenkov signal detected for singly charged particles ($N_0 = 14.7$) and on the resolution of the single photoelectron peak (σ_{pe}). The systematic uncertainty scales with Z , dominates for higher charges and is around 1%. It appears due to non-uniformities at the radiator level coming from variations in the refractive index, tile thickness or clarity or due to non-uniformities at the photon detection efficiency like PMT temperature effects or light guide non-uniformities.

The RICH goal of a good charge separation in a wide range of nuclei charges implies a good mapping and monitoring of the potential non-uniformities present on the detector. In order to keep the systematic uncertainties below 1%, the aerogel tile thickness, the refractive index and the clarity should not have a spread greater than 0.25 mm, 10^{-4} and 5%, respectively; at the detection level a precise knowledge ($< 5\%$ level) of the single unit cell photo-detection efficiency and gains is required.

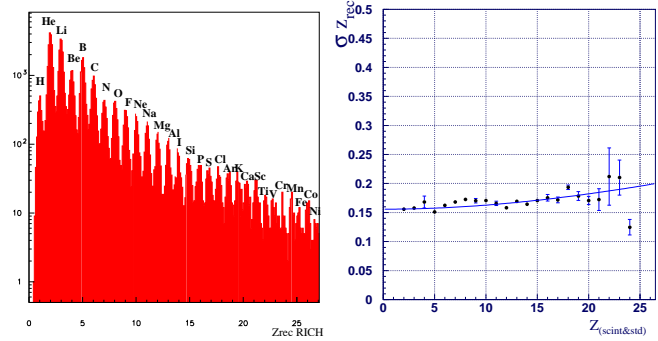


Fig. 7. Charge peaks distribution measured with the RICH prototype using a $n=1.05$ aerogel radiator, 2.5 cm thick. Individual peaks are identified up to $Z = 26$ (left). Charge resolution versus particle Z for the same aerogel radiator. The curve gives the expected value estimated as explained in the text (right).

Runs with a mirror prototype were also performed and its reflectivity was derived from data analysis. The obtained value is in good agreement with the design value.

V. CONCLUSIONS

AMS-02 will be equipped with a proximity focusing RICH detector based on a mixed radiator of aerogel and sodium fluoride, enabling velocity measurements with a resolution of about 0.1% and extending the charge measurements up to the iron element. Velocity reconstruction is made with a likelihood method. Charge reconstruction is made in an event-by-event basis. Evaluation of both algorithms on real data taken with in-beam tests at CERN, in October 2003 was done. The detector design was validated and a refractive index 1.05 aerogel was chosen for the radiator, fulfilling both the demand for a large light yield and a good velocity resolution. The RICH detector is being constructed and its assembling to the AMS complete setup is foreseen for 2008.

REFERENCES

- [1] C. Lechanoine-Leluc, *Proc. 29th ICRC (Pune)* **3**, 381-384 (2005).
- [2] F. Barão, L. Arruda, *et al.*, *Proc. 29th ICRC (Pune)* **9**, 299-302 (2005).
- [3] C. Lechanoine-Leluc, *Proc. 29th ICRC (Pune)* **9**, 299-302 (2005).
- [4] D. Casadei *et al.*, *Nuclear Physics B (Proc. Suppl.)* **113**,133 (2002).
- [5] F. Barao, L. Arruda *et al.*, *NIM* **A502**,310 (2003).
- [6] P. Aguayo, L.Arruda *et al.*, *NIM* **A560**, 291-302 (2006).
- [7] R. Pereira, L.Arruda *et al.*, In-beam aerogel light yield characterization. for the AMS/RICH detector, *AMS internal note in preparation*